SAHC2014 – 9th International Conference on
Structural Analysis of Historical Constructions
F. Peña & M. Chávez (eds.)
Mexico City, Mexico, 14–17 October 2014

MACRO AND MICRO-BLOCK MODELING APPROACHES FOR THE OUT-OF-PLANE LOAD CAPACITY OF A MASONRY WALL WITH TWO SIDEWALLS

Claudia Casapulla[1], Lucrezia Cascini[2], Francesco Portioli[2]

[1] Dept. of Structures for Engineering and Architecture
Via Forno vecchio, 36, Napoli (Italy)
casacla@unina.it

[2] Dept. of Structures for Engineering and Architecture
Via Forno vecchio, 36, Napoli (Italy)
{lucrezia.cascini, fportiol}@unina.it,

Keywords: Limit Analysis, 3D Masonry Systems, Non-associative Friction, Out-of-plane Failure Modes, Macro and Micro Modeling.

Abstract. *In this paper, novel macro and micro-block modeling approaches are adopted for the assessment of the collapse load factor and failure mode of block masonry structures. The out-of-plane behavior of a masonry system composed of a façade wall connected with two sidewalls is investigated by means of limit analysis and some recurrent classes of mechanisms are analyzed. These involve rocking, sliding, torsion failure and combinations of them. Both modeling approaches consider masonry as an assemblage of dry rigid blocks with frictional behavior and non-associative flow rules. The macro-block modeling is based on the assumption that all the possible relative motions among micro-blocks are concentrated along the cracks; assuming maximum and minimum frictional resistances along the cracks, two limiting conditions for the ultimate load factor are kinematically computed by use of minimization routines. The micro-block model is based on a novel numerical strategy to solve the non-associative friction problem; second order cone programming (SOCP) is used to allow the conic yield function to be solved directly. Proper graphics show the obtained results with reference to some given geometric parameters and comparisons between both approaches.*

1 INTRODUCTION

Limit analysis of rigid block assemblages has been found to be a valuable computational tool for the prediction of the collapse load and the failure mechanism of masonry structures, since Kooharian [1] and Heyman [2]. A modeling strategy, which has demonstrated to be useful within this framework, is the combination of block elements, rigid or deformable, with interface elements. This model type is appealing for both micro and macro-modeling. An interesting review of classical and advanced methods was presented by Roca et al. [3].

The use of both macro and micro-modeling in limit analysis become more interesting when the frictional behavior is considered at contact interfaces. In such a case, proper assumptions need to be made on the flow rules to define associative or non-associative solutions. These assumptions involve important implications on the value of collapse load multiplier and the failure mechanism, considering that, generally speaking, non-associated flow rules do not guarantee unique solutions to the limit analysis problems (non-standard limit analysis). The adoption of Coulomb frictional sliding under a normality assumption (associated flow rule) has largely been adopted in the literature [4-13], along with the model under the non-associated flow rule [14-19].

In this paper the computational strategies for macro and micro-block modeling of masonry systems presented in [20-28] are adopted. For both approaches, a rigid-perfectly plastic model with dry contact interfaces governed by Coulomb failure criterion is assumed. Masonry walls with regular units and staggering are concerned. The cracking and crushing of blocks is ignored (these were addressed within micro-block modeling for 2D problems in [29-32]) and the plastic dissipation due to friction is reduced to contact interfaces.

The macro-block model is based on the assumption that the general failure involves a number of cracks, which separate the structure into a few macro-blocks and all the possible relative motions among micro-blocks (units) are concentrated along these cracks. The novel solution procedure is aimed at identifying upper and lower thresholds for the possible collapse load factor by considering how frictional resistances can develop along the crack lines.

Concerning the micro-block modeling approach, a three-dimensional limit analysis model of dry-jointed masonry structures is described. A concave contact formulation is adopted in which contact points are located at the corners of interfaces, allowing failure modes involving opening and sliding to be simulated. An iterative solution procedure is used to solve the non-associative friction problem, with second order cone programming (SOCP) used to allow the conic yield function to be solved directly.

The two novel models are herein used to investigate the most recurrent failure modes of a masonry system composed of a façade wall connected with two sidewalls, i.e.:

- Mechanism 1, characterized by the overturning of a part of the façade wall together with a portion of the sidewalls, involving sliding-rocking failure of the sidewalls (Fig. 1a);
- Mechanism 2, characterized by the overturning of a portion of the sole façade wall, involving twisting-sliding failure of the façade itself (Fig. 1b);
- Mechanism 3, characterized by a mix of Mechanism 1 and Mechanism 2.

In the following sections, both the macro and micro-block models along with the corresponding solution procedures are widely described. Then a parametric analysis has been carried out in order to assess the influence of some geometrical parameter on the prevalence of a specific mechanism over the other.

2 THE MACRO-BLOCK MODELING

The simplified macro-block model and solution procedure recently proposed for in-plane and out-of-plane loaded masonry walls [24, 26] are herein applied to the masonry system under investigation. This is composed of a façade wall connected with two sidewalls which are loaded by the self-weights and horizontal out-of-plane forces proportional to the weights, which simulate the seismic actions.

The Coulomb friction model of dry rigid block masonry with non-standard behavior (non-associative frictional sliding) is adopted and, according to the concept of macro-modeling, it is assumed that the general failure involves a number of cracks, which separate the structures into a few macro-blocks. All the possible relative motions among micro-blocks (units) are concentrated along these cracks which are considered as average inclinations of the discontinuous lines following the disposition of joints which tends to separate the walls in macro-blocks. The geometrical variability of the moving parts of the walls is represented by the variables of the problems, i.e. the height and the inclination of the crack lines. These variables strongly depend on geometrical and mechanical parameters (unit shape ratio, length of the front wall, friction).

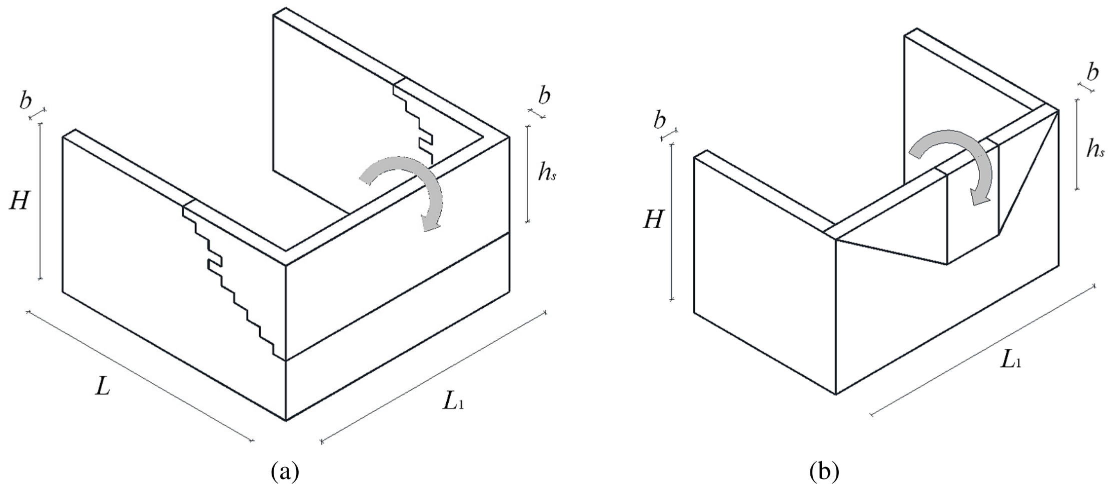

Figure 1: (a) Mechanism 1 with sliding-rocking failure of the sidewalls; (b) Mechanism 2 with twisting-sliding-rocking failure of the front wall.

The proposed solution procedure is based on the computation of a possible range of values for the load multiplier within the maximum and minimum amount of dissipation. The maximum value, i.e. upper bound, corresponds to the hypothesis of full development of the frictional resistance on every bed joint along the crack, whilst the minimum amount, i.e. lower bound, is based on the total absence of friction. In cases where the lower bound is too conservative, little friction could be assumed to narrow the range.

The steps of this solution procedure can be summarized in:

- evaluation of the maximum in-plane and out-of-plane frictional resistances within the walls;
- definition of the inclination and the height of the crack lines corresponding to the minimum kinematic multiplier, based on the hypothesis of the complete activation of frictional resistances along the cracks; such a multiplier represents the upper bound of the range;
- evaluation of the kinematic load factor corresponding to the same crack pattern (say the same height and inclination of the crack lines), but based on the hypothesis of nil activa-

tion of frictional resistances along the same cracks; such a multiplier represents the lower bound of the range.

Actually, the mechanism associated to the upper bound does not correspond to the "exact" one, by its very definition. Nevertheless, it can be used to indicate the prevalence of a failure mode over the other and to recognize the contribution of each parameter to the stability from a geometrical point of view.

2.1 Maximum frictional resistances and ranges of solutions

2.1.1. Mechanism 1

The Mechanism 1 illustrated in Fig. 1a is characterized by the overturning of part of the façade wall together with a portion of the sidewalls, involving frictional resistances along the inclined crack lines. The system is loaded by the self-weight and horizontal out-of-plane forces proportional to the weights, simulating seismic actions and parallel to the plane of the sidewalls.

Having assumed the same thickness for all the walls, the geometrical parameters influencing the out-of-plane load capacity are the shape ratio of the units s/h and the length of the front wall L_1, while the wall height H and the length L of the sidewalls are irrelevant, provided that $h_s \leq H$ and $\alpha_b \leq \alpha_p$ (Figs. 1, 2). The other meaningful parameter is the friction coefficient.

The frictional resistances are represented by shear forces acting on the plane of the sidewalls. With reference to the single sidewall in Fig. 2a, the maximum frictional force arising in its plane, based on the hypothesis of complete activation of frictional resistances along the crack, is given by the product of the weight of trapezoid OABC times the friction coefficient f [24, 26]:

$$F = \frac{(h_s \tan\alpha_b + 2b - s)h_s}{2}\gamma b f \qquad (1)$$

where γ is the specific weight of the material and the geometrical parameters are represented in Figs. 1 and 2.

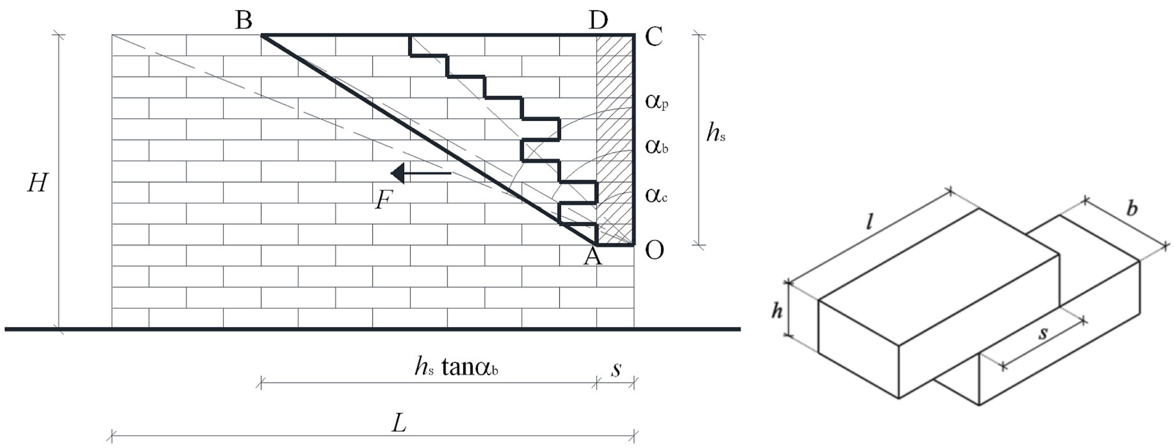

Figure 2: (a) Sidewall with inclinations for the unit (α_b) and wall shape (α_p) ratios and for the variable angle of crack (α_c). (b) Unit dimensions.

According to the developments presented in [26], it is easy to verify that the virtual work equation for incipient overturning yields:

$$\lambda_1 \frac{Ph_s}{2} + 2\lambda_1 P_1 \frac{2}{3} h_s = P\frac{b}{2} + 2P_1\left(\frac{h_s \tan\beta_1}{3} + b\right) + F\frac{2h_s}{3} \tag{2}$$

where P and P_1 are the self-weights of the portions OADC and ABD, respectively, and $\tan\beta_1$ represents the inclination of the crack line with respect to the vertical axis.

Moreover, $\tan\beta_1$ and h_s are the two variable parameters and λ_1 is the load factor of the horizontal external forces. Minimizing λ_1 with respect to those two variables must respect the variability of parameter $\tan\beta_1$ from zero to the maximum inclination given by the staggering ratio and the height of the crack limited to the height of the wall, i.e.:

$$0 \le \tan\beta_1 \le \tan\beta_{max}; \qquad h_s \le H \tag{3}$$

where $\tan\beta_{max} = (h_s \tan\alpha_b - s)/h_s$.

Also horizontal equilibrium must be guaranteed and so it is further required that:

$$\lambda_1 (P + 2P_1) = 2F \tag{4}$$

On the other hand, it is known that the "exact" load factor cannot be larger than the friction coefficient, i.e. $\lambda_1 \le f$ and when $\lambda = f$ only pure sliding can occur. So, once defined the values of $\tan\beta_1$ and h_s which minimize λ_1 and satisfy Eqs. (3) and (4), the upper threshold is obtained. On the other hand, the lower threshold for the same crack pattern, i.e. the same values of h_s and $\tan\beta_1$, is simply obtained from Eq. (2) setting the frictional force equal to zero.

2.1.2. Mechanism 2

Mechanism 2 illustrated in Fig. 1b represents the failure of the façade wall constrained at two sidewalls and loaded by the self-weight and horizontal out-of-plane forces proportional to the weights, simulating seismic actions. The latter can be oriented both inward and outward, with the assumption that, if outward, the overturning of the entire wall, due to the yielding of the sidewall capacity, is prevented. In order to be triggered, the mechanism must also satisfy the condition whereby the resistance to the outward displacement, developed by the edges of the façade, is overcome. That is to say, the arch effect in the façade wall is negligible.

The crack pattern of this mechanism is characterized by three macro-blocks separated by cylindrical hinges and with variable height x. The frictional resistances arising along the vertical and diagonal crack lines are represented by interactions of shear forces and torsion moments. For this case, the yield functions for pure shear, pure torsion and their interaction firstly proposed by Casapulla [33] are herein adopted.

It easy to verify [26] that the virtual work equation for incipient collapse can be solved for the load factor λ_2 in the form:

$$\lambda_2 = \frac{3\left[bL_2^2 h(2P_2 + P_3) + 8P_2 sfd_0 x^2\right]}{[(4P_2 + 3P_3)L_2 + 12d_0(P_2 + P_3)]xhL_2} \tag{5}$$

where P_2 and P_3 are the self-weights of the triangular and rectangular macro-blocks, respectively, and d_0 is the torsion constant.

The upper threshold of the "exact" collapse load factor is obtained from minimization of Eq. (5) with respect to x, also satisfying the condition $\lambda_2 \le f$. Moreover, the lower threshold for the same crack inclination, i.e. the same value of x, is simply obtained from Eq. (5) setting the friction coefficient equal to zero.

3 THE MICRO-BLOCK MODELING

A recently proposed formulation [26, 34] within the framework of non-standard rigid block limit analysis [10-19] is herein adopted. This is based on a concave contact formulation and conic yield surface for Coulomb friction. An iterative solution procedure is adopted to solve the non-associative friction problem, with second order cone programming (SOCP) used to allow the conic yield function to be solved directly.

To investigate the three-wall masonry system under study, a fictitious zero angle of friction is used to take into account non-associative behavior in sliding and the rigid blocks are assumed to interact through bed joints only. Three numerical models are considered:

- Mechanism 1, named Num_M1, where the twisting about vertical axis of the interfaces has been locked in order to prevent the out-of-plane failure of the sole façade wall;
- Mechanism 2, named Num_M2, which is constrained to horizontal displacements at two edges in order to prevent the overturning of the façade wall due to the yielding of the sidewall capacity;
- Mechanism 3, named Num_M3, where all constraints are relaxed in order to simulate the out-of-plane failure as a combination of Mechanism 1) and Mechanism 2).

The implemented formulation for micro-modeling is based on the iterative solution of cone programs according to the lower bound theorem of limit analysis and stated as follows:

$$\begin{aligned} &\mathit{max} && \lambda \\ &\mathit{subjected\ to:} && \mathbf{A}\,\mathbf{x} = \mathbf{f} \\ & && \mathbf{x} \in \boldsymbol{C}_\mathbf{0} \end{aligned} \tag{6}$$

In this formulation λ is the collapse load multiplier and the two relations express the equilibrium and yield conditions of the 3D rigid block assemblage in matrix form, respectively. In particular, **x** is the vector of the internal static variables at contact interfaces, **A** is the equilibrium matrix, **f** is the vector of external loads and $\boldsymbol{C}_\mathbf{0}$ is the convex cone yield function matrix. Matrices and vectors for the whole rigid block assemblage are assembled from matrices and vectors referred to each unit and contact interface (Fig. 3).

According to concave formulation, the behavior at each interface is fully represented if yield functions for opening and sliding are defined at the four contact points located at the corners of the interface itself. The yield function matrix $\boldsymbol{C}_\mathbf{0}$ is thus assembled on the basis of these yield functions which take into account sliding and opening failure modes.

For each contact k, sliding is governed by a Coulomb-type criterion. This can be represented by a cone yield function in the three-dimensional space of normal force N_k and shear components T_{1k} and T_{2k}. This yield function can be expressed in the form:

$$y_k^s = \sqrt{T_{1k}^2 + T_{2k}^2} - f\,N_k \leq 0 \tag{7}$$

where f is the friction coefficient taken as constant for all contact interfaces.

For normal forces, under the assumption of infinite compressive strength and tensionless behavior, the following yield functions have been considered.

$$y_k^O = -N_k \leq 0 \tag{8}$$

These yield functions simply express the condition that normal forces at contact points must be non-negative.

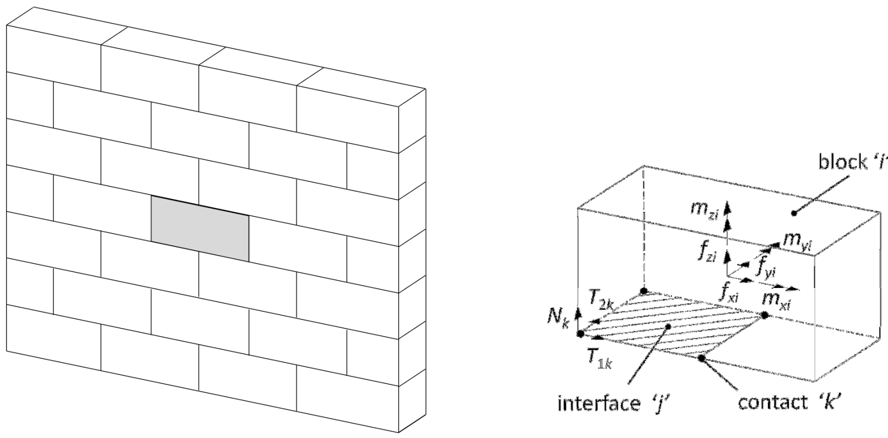

(a) (b)

Figure 3: (a) Micro-block model; (b) static variables at block centroid *i*, and contact point *k*.

3.1 Iterative procedure for non-associative frictional behavior

The procedure to take into account non-associative frictional behavior consists in the solution of a series of cone programming sub-problems, formulated according to (6).

The first step of the procedure is the associative solution obtained by solving standard limit analysis problem so as to calculate the initial values of normal forces. In this step the problem is formulated assuming nil value of cohesion and considering the effective value of friction angle. Then, a fictitious zero value of friction angle and a fictitious cohesion are used to rotate the yield surface orientation so as to restore the normality to the model and to improve the convergence of the procedure. This implies that sliding behavior at contacts is governed at each iteration by a cylindrical failure surface with an effective cohesion intercept but a zero angle of friction.

The iterative procedure for non-associated flow rule stops when the prescribed convergence tolerance is reached, that is when:

$$\frac{\left|\lambda_{\text{iter}} - \lambda_{\text{iter}-1}\right|}{\lambda_{\text{iter}}} \leq \text{tol} \tag{9}$$

Displacements of blocks and contact strain rates are obtained from the solution of the dual cone program, corresponding to the kinematic formulation of the limit analysis problem.

The algorithm developed can be summarized as follows:

- Set the SOCP problem according to (6), solve and get load multiplier λ_{ass} and normal forces for associative friction solution.
- Start iterative procedure to take into account non-associative behavior in sliding; set iteration number iter=1.
- Define new sliding friction failure criteria for the next iterations on the basis of calculated normal forces and the algorithm parameter.
- Solve the SOCP problem, get load multiplier λ_{iter} and normal forces.
- If $\frac{\left|\lambda_{\text{iter}} - \lambda_{\text{iter}-1}\right|}{\lambda_{\text{iter}}} \leq$ tolerance, then iter=iter+1 and repeat from step 3); else exit.

Get displacements **u** from the dual SOCP problem (6).

4 DISCUSSION OF THE RESULTS

The influence of some geometrical and mechanical parameters on the out-of-plane mechanisms under study are investigated in this section and the results obtained by both macro and micro-block modeling approaches are compared each other. The analyzed parameters are the size ratio of the front wall and the unit aspect ratio, indicated by the following non-dimensional variable, respectively:

$$D_1 = \frac{L_1}{l}; \quad C = \frac{s}{h} \tag{10}$$

Considering the sidewalls with the same thickness as the front wall, the other fixed parameters are:

$$B_1 = \frac{b}{l} = 0.5; \qquad f = 0.7 \tag{11}$$

The wall height is irrelevant, provided that it is larger than x and h_s (the heights of the moving parts of the walls).

4.1 Size ratio

The effect of the size ratio is first investigated with reference to the micro-block model only. Fig. 4a shows that the load factors for all mechanisms decrease with increasing D_1. It also highlights that the curves corresponding to the two mechanisms Num_M1 and Num_M2 always overestimate the out-of-plane capacity of the system represented by Num_M3 and tend to it for very short and very long front walls. In particular, Num_M1 appears to be prevalent to Num_M2 up to $D_1 \approx 8.8$ while for longer walls the prevalent mechanism will be M2.

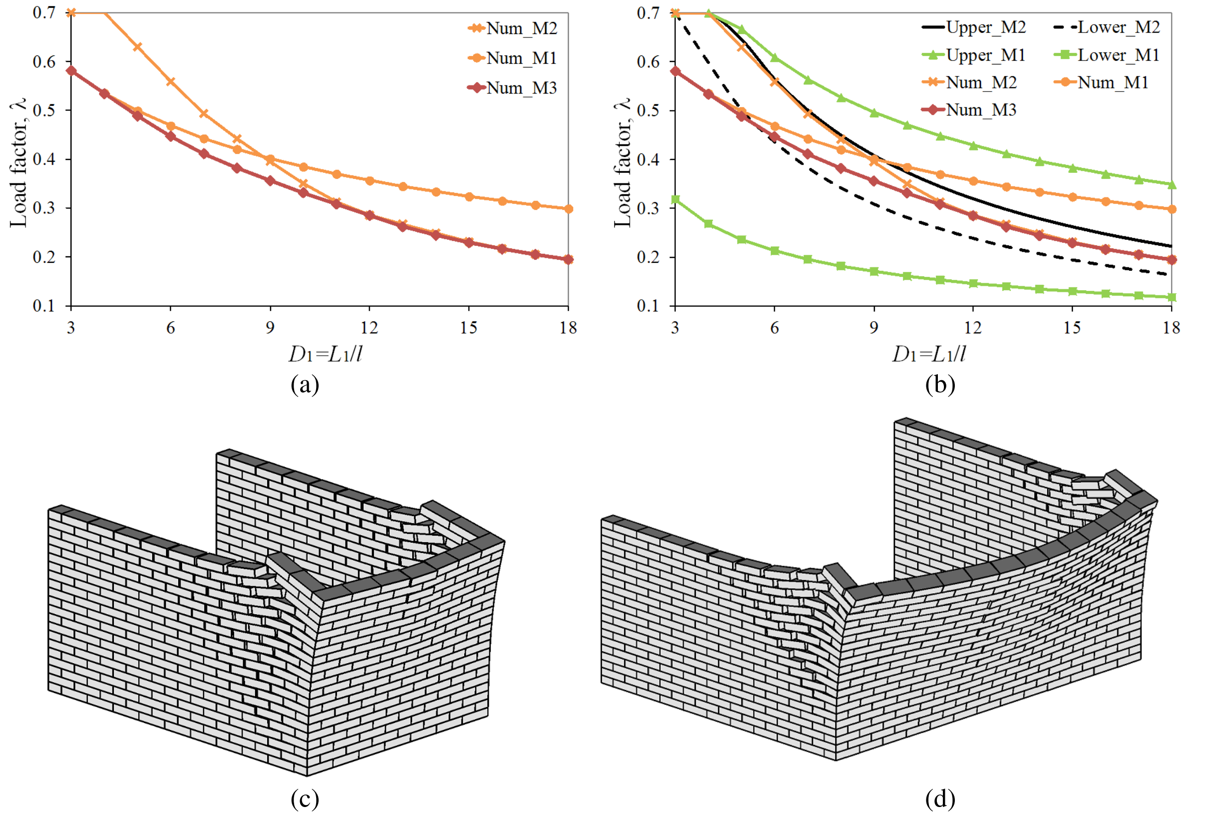

Figure 4: Size ratio effect. Load factors vs. size ratio of the front wall for (a) micro-block model, (b) micro and macro-block models. Micro-block failure mechanisms for M3, with (c) D_1 = 7 and (d) D_1 = 13.

This trend is also confirmed in terms of failure modes. In fact, for shorter front walls ($D_1 = 7$) mechanism M1 has a shape similar to M3 (Fig. 4c), while for longer walls ($D_1 = 13$) the mechanism closer to M3 (Fig. 4d) appears to be M2.

Concerning the macro-block modeling approach, although the prevalence of a mechanism over the other cannot be derived in such a simple manner, a reliable range of solutions containing the numerical results Num_M3 may be found. In Fig. 4b the green curves, named Upper_M1 and Lower_M1, and the black curves, named Upper_M2 and Lower_M2, are represented to bound the solutions for M1 and M2, respectively. It is expected that the likely "exact" solution is bounded from above by the minimum values between Upper_M1 and Upper_M2 and from below by the minimum values between Lower_M1 and Lower_M2. The so defined range is characterized by Upper_ M2 and Lower_M1, but it could be in some cases too large from an engineering perspective. However, as the bounds for M2 are fully contained in the range for M1 and contain the curve Num_M3 for almost all values of D_1, these may be assumed as a narrower range for such classes of mechanisms.

4.2 Unit aspect ratio

Figures 5a,b show the results for both modeling approaches, in terms of load factor in function of the unit aspect ratio C for two different values of D_1.

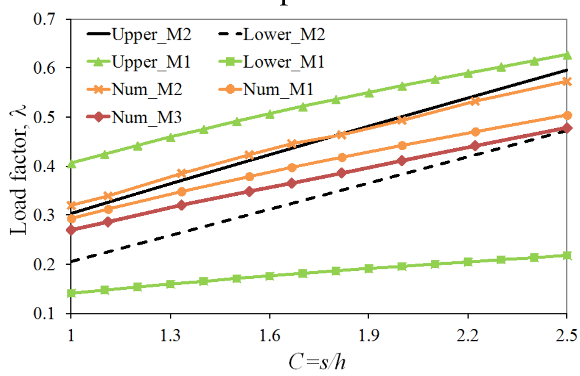

(a)

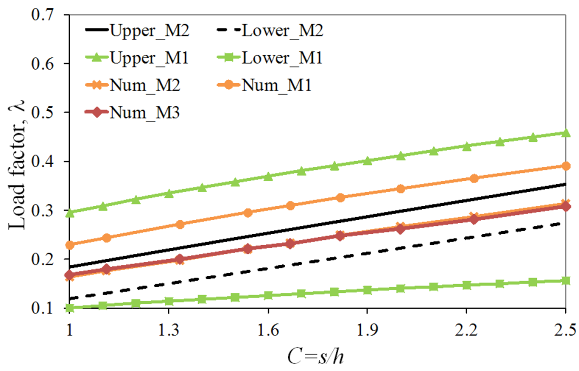

(b)

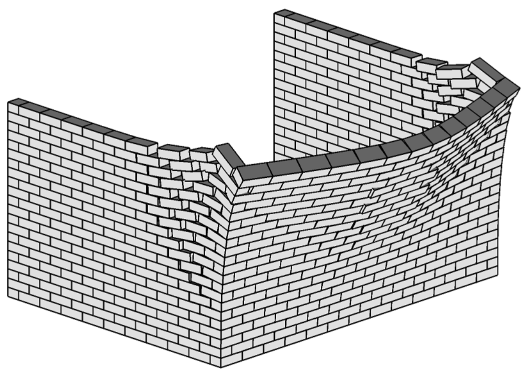

(c)

Figure 5: Unit aspect ratio effect. Load factors vs. unit aspect ratio for (a) $D_1 = 7$ and (b) $D_1 = 13$. (c) Micro-block failure mechanisms for M3, with $D_1 = 13$ and $C = 1.5$.

It is first evident that all curves are influenced by parameter C in an almost proportional way and that the prevalence of a mechanism over the other is indicated by the distances of their values from the results for M3. In fact, it can be observed that for $D_1 = 7$ (Fig. 5a) the curve Num_3 is closer to Num_M1 than to Num_M2, whatever the value of unit aspect ratio. The opposite situation can be predicted for longer front walls, e.g. for $D_1 = 13$ (Fig. 5b), for which Num_M2 is coincident with Num_M3 in nearly every case. This result confirms the trend already observed in Fig. 4a, i.e. the prevalent failure mode is M1 for shorter front walls and M2 for longer ones. Also, it is confirmed that, whatever the value of C, the numerical results corresponding to the two mechanisms M1 and M2 always overestimate the out-of-plane capacity of the system represented by M3.

Regarding the results obtained by macro-block modeling approach, a reliable range of solution in function of the unit shape ratio is still represented by the range for M2, in analogy to what described for parameter D_1. In fact, it always contains the curve related to Num_M3, whatever the value of C, as shown in Figs. 5a,b for shorter (D_1 = 7) and longer (D_1 = 13) façade walls, respectively.

By comparing the results in terms of failure modes, it is clear that the prevalence of a mechanism over the other is not affected by parameter C. In fact, it resulted that e.g. for a system with long façade wall (D_1 = 13) mechanism M2 has a shape similar to M3 (Fig. 5c) for both thickset (C = 1.5) and slender units (C = 2.5).

5 CONCLUSIONS

The limit analysis of a masonry system composed of a façade wall connected with two sidewalls was carried out in this paper by adopting novel macro and micro-block models and solution procedures within three-dimensional limit analysis. A rigid-perfectly plastic model with dry contact interfaces governed by Coulomb failure criterion was assumed for masonry walls with regular units and staggering (non-standard limit analysis). Three classes of out-of-plane failure modes were investigated, involving rocking, sliding, torsion failure and combinations of them.

As far as the macro-modeling approach is concerned, reliable ranges of existence for the collapse load factors and indications for the crack patterns were discussed with reference to two recurrent classes of out-of-plane failure modes. Instead, an iterative procedure based on the formulation of conic sub-problems has been used within the micro-block modeling approach to take into account non-associative frictional behavior at contact interfaces and three failure modes were investigated.

Then, a parametric analysis was carried out to compare the results obtained by the two proposed methods of analysis and to derive interesting remarks on some influencing parameters. In particular, while the prevalence of Mechanism 1 over the Mechanism 2 and vice versa is mostly influenced by the length of the façade wall, the unit aspect ratio only affects the global resistance and the portion of masonry involved in the mechanism.

Analyzing numerical results it can be derived that Mechanism 1 is prevalent for systems with shorter front walls, while Mechanism 2 is prevalent for longer ones. Both mechanisms always overestimate the out-of-plane capacity of the system represented by Mechanism 3 which is assumed to be a mix between them. Also, for all the cases examined a reliable narrow range for the load multiplier was obtained using macro-block analysis which nearly always contains the numerical results for Mechanism 3 (micro-block model).

In order to assess the seismic risk for masonry buildings, the proposed procedures can easily be extended to other classes of out-of-plane mechanisms, which can then be investigated in static and dynamic fields by means of other methods of analysis [35, 36].

ACKNOWLEDGMENTS

The authors acknowledge the sponsorship of the Italian Civil Protection, through the RELUIS Project - Line: Masonry Structures (2014).

REFERENCES

[1] A. Kooharian, Limit analysis of voussoir (segmental) and concrete arches. *Journal of American Concrete Institute*, **24**(4), 317-328, 1952.

[2] J. Heyman, The stone skeleton. *International Journal of Solids and Structures*, **2**, 249-279, 1966.

[3] P. Roca, M. Cervera, G. Gariup, L. Pela', Structural Analysis of Masonry Historical Constructions. Classical and Advanced Approaches. *Archives of Computational Methods in Engineering*, **17**, 299-325, 2010.

[4] J.M. Delbecq, Analyse de la stabilité des voûtes en maçonnerie par le calcul á la rupture. *Journal De Mécanique théorique et appliquée*, **1**, 91-121. 1982.

[5] R.K. Livesley, A computational model for the limit analysis of three-dimensional masonry structures, *Meccanica*, **27**(3), 161-172, 1992.

[6] A. Giuffrè, *Guide to the seismic retrofit project*, In: *Safety and Conservation of Historical Centres: The Ortigia Case*. Laterza Ed., Bari, Italy, pp. 151-188, 1993. (in Italian)

[7] M. Gilbert, C. Melbourne, Rigid-block analysis of masonry structures. *The Structural Engineer*, **72**, 356-361, 1994.

[8] T.E. Boothby, Stability of masonry piers and arches including sliding. *Journal of Engineering Mechanics*, **120**, 304-319, 1994.

[9] C. Casapulla, Dry rigid block masonry: Safe solutions in presence of Coulomb friction. *Advances in Architecture Series*, **7**, 251-261, 2001.

[10] F. Portioli, C. Casapulla, L. Cascini, M. D'Aniello, R. Landolfo, Limit analysis by linear programming of 3D masonry structures with associative friction laws and torsion interaction effects. *Archive of Applied Mechanics*, **83**(10), 1415-1438, 2013.

[11] F. Portioli, C. Casapulla, L. Cascini, R. Landolfo, Three-Dimensional Limit Analysis of Dry-Joint Masonry Walls using Rigid Block Modelling. *14th International Conference on Civil, Structural and Environmental Engineering Computing (Civil-Comp 2013)*, Cagliari, Sardinia, Italy, pp. 1-14, September 3-6, 2013.

[12] F. Portioli, C. Casapulla, L. Cascini, M. D'Aniello, R. Landolfo, Three-Dimensional Limit Analysis of Dry-Joint Masonry Walls by Rigid Block Modelling Using Linear Programming. *2nd International Conference on Protection of Historical Constructions (PROHITECH14)*, Antalya, Turkey, pp. 187-192, May 7-9, 2014.

[13] F. Portioli, C. Casapulla, L. Cascini, Application of a three-dimensional rigid block model to the limit analysis of large scale masonry panels. *12th International Conference on Computational Structures Technology (CST2014)*, Naples, Italy, September 2-5, 2014.

[14] D.W. Begg, R.J. Fishwick, Numerical analysis of rigid block structures including sliding. *3rd International Symposium on Computer Methods in Structural Masonry (STRUMAS III)*, Lisbon, Portugal, Vol. 3, pp. 177-183, April, 1995.

[15] C. Baggio, P. Trovalusci, Collapse behaviour of three-dimensional brick-block systems using non-linear programming. *Structural Engineering and Mechanics*, **10**(2), 181-195, 2000.

[16] M. Ferris, F. Tin-Loi, Limit analysis of frictional block assemblies as a mathematical program with complementarity constraints. *International Journal of Mechanical Sciences*, **43**, 209-224, 2001.

[17] A. Orduña, P.B. Lourenço, Cap model for limit analysis and strengthening of masonry structures. *Journal of Structural Engineering-ASCE*, **129**(10), 1367-1375, 2003.

[18] A. Orduña, P.B. Lourenço, Three-dimensional limit analysis of rigid blocks assemblages. Part I: torsion failure on frictional interfaces and limit formulation. International *Journal of Solids and Structures*, **42**, 5140-5160, 2005.

[19] M. Gilbert, C. Casapulla, H.M. Ahmed, Limit analysis of masonry block structures with non-associative frictional joints using linear programming. *Computers and Structures*, **84**(13-14), 873-887, 2006.

[20] C. Casapulla, D. D'Ayala, In-plane collapse behaviour of masonry walls with frictional resistances and openings. 5th International Conference (SAHC06), New Delhi, India, vol. 2, pp 1159-1166, November 6-8, 2006.

[21] C. Casapulla, Lower and upper bounds in closed form for out-of-plane strength of masonry structures with frictional resistances. *6th International Conference (SAHC08)*, Bath, UK, vol. 2, pp. 1191-1198, July 2-4, 2008.

[22] C. Casapulla, A. Maione, Out-of-plane local mechanisms in masonry buildings. The role of the orientation of horizontal floor diaphragms. *9th Australasian Masonry Conference, Queenstown, New Zealand*, February 15-18, pp. 225-235, 2011.

[23] C. Casapulla, F. Portioli, A. Maione, R. Landolfo, Macro and micro-block modelling for limit analysis of masonry structures with non-associative frictional joints. *8th International Conference on Structural Analysis of Historical Constructions (SAHC12)*, Wroclaw, Poland, pp. 441-448, October 15-17, 2012.

[24] C. Casapulla, F. Portioli, A. Maione, R. Landolfo, A macro-block model for in-plane loaded masonry walls with non-associative Coulomb friction. *Meccanica*, **48**(9), 2107-2126, 2013.

[25] M. Sassu, M. Andreini, C. Casapulla, A. De Falco, Archaeological consolidation of UNESCO masonry structures in Oman: the Sumhuram Citadel of Khor Rori and the Al-Balid Fortress. *International Journal of Architectural Heritage*, **7**(4), 339-374, 2013.

[26] C. Casapulla, L. Cascini, F. Portioli, R. Landolfo, 3D macro and micro-block models for limit analysis of out-of-plane loaded masonry walls with non-associative Coulomb friction". *Meccanica*, **49**(5), 1653-1678, 2014.

[27] C. Casapulla, F. Portioli, A. Maione, R. Landolfo, Non-standard limit analysis for in-plane loaded masonry walls. *2nd International Conference on Protection of Historical Constructions (PROHITECH14)*, Antalya, Turkey, pp. 193-199, May 7-9, 2014.

[28] C. Casapulla, F. Portioli, L. Cascini, Non-standard Limit Analysis of 3D Masonry Systems subjected to Out-of-plane Loading. *12th International Conference on Computational Structures Technology (CST2014)*, Naples, Italy, September 2-5, 2014.

[29] F. Portioli, L. Cascini, L., M. D'Aniello, R. Landolfo, A Rigid Block Model with Cracking Units for Limit Analysis of Masonry Walls subject to In-Plane Loads. *11th International Conference on Computational Structures Technology (CST 2012)*, Dubrovnik, Croatia, pp. 1-8, September 4-7, 2012.

[30] F. Portioli, L. Cascini, C. Casapulla, M. D'Aniello, Limit analysis of masonry walls by rigid block modelling with cracking units and cohesive joints using linear programming. *Engineering Structures*, **57**, 232-247, 2013.

[31] F. Portioli, L. Cascini, C. Casapulla, M. D'Aniello, Computational limit analysis of masonry panels with cracking units using rigid block modelling. *14th International Conference on Civil, Structural and Environmental Engineering Computing (Civil-Comp 2013)*, Cagliari, Sardinia, Italy, pp. 1-10, September 3-6, 2013.

[32] F. Portioli, L. Cascini, C. Casapulla, M. D'Aniello, R. Landolfo, Limit analysis of confined masonry shear walls by rigid block modeling with cracking units. *8th International Conference on Structural Analysis of Historical Constructions (SAHC12)*, Wroclaw, Poland, pp. 534-40, October 15-17, 2012.

[33] C. Casapulla, Resistenze attritive in una parete muraria soggetta ad azioni normali al suo piano medio. *9th National Conference (Anidis99)*, Torino, Italy, September 20-23, 1999. (CD-R, in Italian)

[34] F. Portioli, C. Casapulla, M. Gilbert, L. Cascini, Limit analysis of 3D masonry block structures with non-associative frictional joints using cone programming. *Computers and Structures*, **143**, 108-121, 2014.

[35] C. Casapulla, P. Jossa, A. Maione, Rocking motion of a masonry rigid block under seismic actions: A new strategy based on the progressive correction of the resonance response. *Ingegneria Sismica*, **27**(4), 35-48, 2010.

[36] C. Casapulla, A. Maione, L.U. Argiento, A simplified approach for the seismic vulnerability assessment: application to a masonry building in Naples. *9th International Conference on Structural Analysis of Historical Constructions (SAHC14)*, Mexico City, Mexico, October 14-17, 2014.